Comparison of Controllable Transmission Ratio Type Variable Stiffness Actuator with Antagonistic and Pre-tension Type Actuators for the Joints Exoskeleton Robots

Hasbi Kizilhan, Ozgur Baser, Ergin Kilic and Necati Ulusoy
Süleyman Demirel University, Mechanical Engineering Departmant, Isparta, Turkey

Keywords: Exoskeleton Robots, Variable Stiffness Actuators, Controllable Transmission Ratio Type Actuators, Antagonistic Type Actuators, Pre-tension Type Actuators.

Abstract: Exoskeleton robots are used as assistive limbs for elderly persons, rehabilitation for paralyzed persons or power augmentation purposes for healthy persons. The similarity of the exoskeleton robots and human body neuro-muscular system maximizes the device performance. Human body neuro-muscular system provides a flexible and safe movement capability with minimum energy consumption by varying the stiffness of the human joints regularly. Similar to human body, variable stiffness actuators should be used to provide a flexible and safe movement capability in exoskeletons. In the present day, different types of variable stiffness actuator designs are used, and the studies on these actuators are still continuing rapidly. As exoskeleton robots are mobile devices working with the equipment such as batteries, the motors used in the design are expected to have minimal power requirements. In this study, antagonistic, pre-tension and controllable transmission ratio type variable stiffness actuators are compared in terms of energy efficiency and power requirement at an optimal (medium) walking speed for ankle joint. In the case of variable stiffness, the results show that the controllable transmission ratio type actuator compared with the antagonistic design is more efficient in terms of energy consumption and power requirement.

1 INTRODUCTION

Human neuro-musculo-skeletal system achieves a flexible and stable walking with minimum energy consumption by changing the stiffness and damping in lower limb joints. The design of exoskeleton robots employing variable stiffness actuators (VSA) has been introduced to the literature in recent time. As exoskeleton robots are mobile robots and interacting with human limbs, variable stiffness actuators used in their designs need to be energy efficient and safe. Utilizing stiff actuators (electricity motor and hydraulic actuators etc.) on these robots is not appropriate to increase safety and provide biomimetic motion. Instead, novel promising designs of variable stiffness actuators are needed to achieve the desired criteria. Due to the significant properties of the variable stiffness actuators like minimizing large shock forces, safely interacting with the user and storing/releasing energy in their passive elastic elements, the use of them on the exoskeleton robots is increasing more and more. Therefore, the studies on novel actuator designs are still continuing rapidly. There are some important design criteria for VSAs. They can be summarized as follows: (1) variable stiffness actuators should be compact and light, (2) stiffness range of the actuators should be wide as possible in order to employ them in many applications, (3) stiffness of the actuators should be changed rapidly, (4) they should have a minimum level of power requirement, (5) both equilibrium position and stiffness of the actuators should be adjusted independently.

Variable stiffness actuator designs (compliant actuators) have considerable advantages such as storing/releasing energy by means of the passive elastic elements used in their structure, safely interacting with the users and minimizing the large shock forces (Alexander, 2010). Therefore, they are started to use in the robots interact with human and humanoid robots. Nowadays, the studies for more efficient, more compact and lighter new actuator designs are still carrying on. These actuators are classified under five different categories. These are equilibrium-controlled, antagonistic-controlled, structure-controlled, mechanically controlled and

Kizilhan H., Baser O., Kilic E. and Ulusoy N..
Comparison of Controllable Transmission Ratio Type Variable Stiffness Actuator with Antagonistic and Pre-tension Type Actuators for the Joints Exoskeleton Robots.
DOI: 10.5220/0005507801880195
In *Proceedings of the 12th International Conference on Informatics in Control, Automation and Robotics* (ICINCO-2015), pages 188-195
ISBN: 978-989-758-123-6

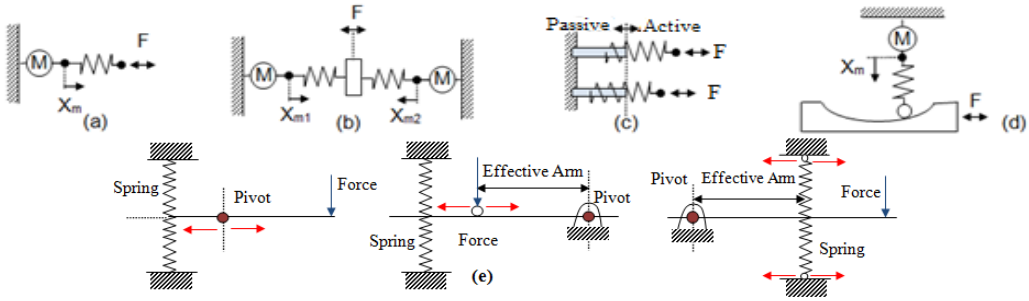

Figure 1: Variable stiffness actuator types: (a) equilibrium-controlled, (b) antagonistic-controlled, (c) structure-controlled, (d) mechanically-Controlled and (e) controllable transmission ratio type actuators.

controllable transmission ratio type actuators (Van Ham, 2007; Vanderborght, 2012). Figure 1 shows their schematic views. Some implementations of these actuators are presented in the references (Pratt, 1995; Migliore, 2005; Hollander, 2006; Jafari, 2010; Jafari, 2011).

2 CONTROLLABLE TRANSMISSION RATIO TYPE, ANTAGONISTIC AND PRE-TENSION ACTUATOR DESIGNS

In this section, all equations are derived to compare antagonistic, pre-tension and controllable transmission ratio type actuators in a simulation study. Firstly, it is assumed that the actuators are designed linearly, and thus the linear motion of the actuators need to be transformed into the rotary motion for lower limb joints. Besides, biomechanical moment and angle data cannot be used directly for linear actuator designs. They should be converted for linear actuator designs according to the mechanism used in the design. A slider-moment arm mechanism can be used for that purpose. Figure 2 shows a schematic drawing of that mechanism applied on the ankle joint so that the rotary motion of the ankle joint can be transformed to a linear motion. The transformation equation of that mechanism can be derived as Eq.(1) by using the trigonometric relation between the ankle joint axis and force application point of the linear actuator.

$$K_{yank} = \frac{\theta_{ank}[cos(\theta_{ank})]^2}{L^2} K_{\theta_{ank}} \quad (1)$$

θ_{ank}, T_{ank}, y_{ank}, F_{ank} in the equations represent ankle joint angle, ankle joint moment, vertical deflection of the linear actuator and output force of the linear actuator, respectively.

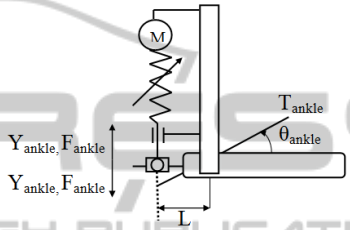

Figure 2: Slider-moment arm mechanism of a linear variable stiffness actuator used in an ankle joint.

2.1 Controllable Transmission Ratio Type Actuator

The stiffness of this type of actuator design is adjusted by changing the transmission ratio between the spring and output link. One motor (M2) performs this stiffness adjustment and another motor (M1) only controls the equilibrium position of the whole mechanism. In this arrangement, as the spring is not forced, no energy is required to change the stiffness of the design. In the design of controllable transmission ratio type actuators presented in this paper, the pivot point and spring position are stationary and the position of the force output link is controlled, and thus the stiffness of the actuator can be tuned to a desired value. Figure 3 shows the schematic view of the presented design. The equivalent output stiffness characteristics of the variable stiffness actuators is desired to be almost linear, so that the elastic elements used in this design need to be linear spring.

As the spring elements used in the design are linear springs, the force output of the actuator can be formulated as Eqs. (2) and (3). The positon of the force output link on the lever arm is changed to adjust the transmission ratio in the controllable transmission ratio type actuator. Figure 4 shows the free body diagram of the lever arm used in the design.

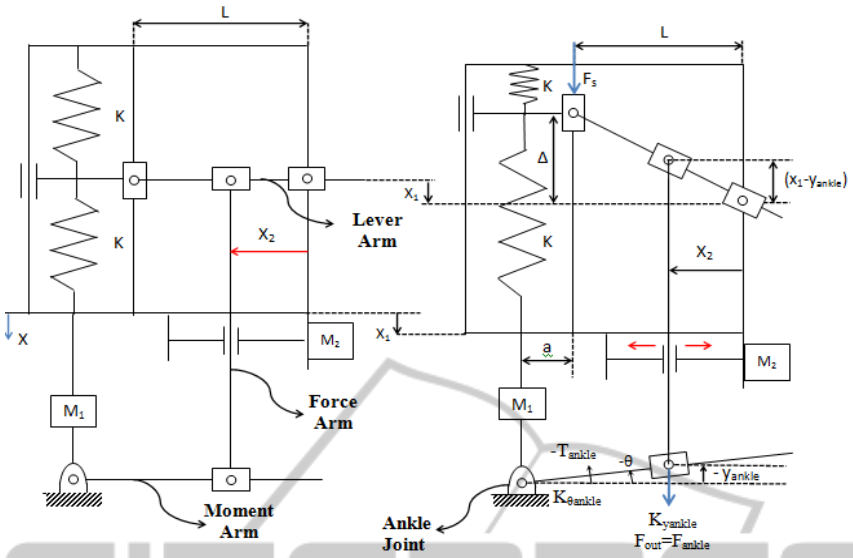

Figure 3: Schematic view of a controllable transmission ratio type actuator.

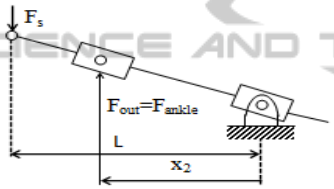

Figure 4: Free body diagram of the lever arm.

$$F_{ank} = -F_{out} = K_{yank}(x_1 - y_{ank}) \quad (2)$$

$$F_{ank} = \frac{LF_s}{x_2} \quad (3)$$

F_{ank}, F_s, L and x_2 in this equation represent the output force of variable transmission mechanism, spring force, horizontal length of the lever arm and the distance between the pivot point and output force link, respectively. Eq.(4) represents the spring force;

$$F_s = 2K\Delta \quad (4)$$

K and Δ in this equation represent the linear spring constant and deflection of springs. Substituting Eq. (4) into the Eq. (3), the output force of the actuator and deflection of the spring can be formulated as Eqs. (5) and (6), respectively.

$$F_{ank} = \frac{2LK\Delta}{x_2} \quad (5)$$

$$\Delta = \frac{L(x_1 - y_{ank})}{x_2} \quad (6)$$

Substituting Eq. (5) into Eq. (6), output force of the actuator can be expressed as follow;

$$F_{ank} = 2.K(x_1 - y_{ank})\frac{L^2}{{x_2}^2} \quad (7)$$

Output force of the actuator is also called as ankle force in the paper. By solving Eq. (2) and (7) in common, the stiffness on the output link (force arm) of the linear actuator can be formulated as Eq. (9);

$$K_{yank}(x_1 - y_{ank}) = 2K(x_1 - y_{ank})\frac{L^2}{{x_2}^2} \quad (8)$$

$$K_{yank} = 2K\frac{L^2}{{x_2}^2} \quad (9)$$

The relation between the ankle force applied by the actuator force arm and ankle moment on the moment arm is depicted in Figure 5. $(a+L-x_2)$ on the figure represents the effective length of the moment arm, and a and L distances are constant according to the controllable transmission ratio type actuator design as shown in Figure 3. x_2 represents the required distance between the output link and pivot point to adjust the stiffness. Besides, θ and y_{ank} represent the ankle joint angle and vertical deflection of the force arm of the actuator, respectively.

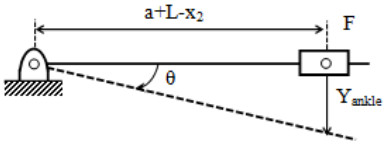

Figure 5: Moment arm mechanism of the ankle joint.

Trigonometric relation between vertical deflection of the force arm (y_{ank}) and ankle joint angle (y_{ank}) can be written as Eqs. (10) and (11) by considering Figure 5.

$$tan\theta = \frac{y_{ank}}{a + L - x_2} \quad (10)$$

$$y_{ank} = (a + L - x_2)tan\theta \quad (11)$$

Also, the relation between the output force of the actuator (ankle force) and ankle moment can be written as Eqs. (12) and (13);

$$T_{ank} = (a + L - x_2)F_{ank} \quad (12)$$

$$T_{ank} = (a + L - x_2)(x_1 - y_{ank})K_{yank} \quad (13)$$

Substituting the trigonometric equation, Eq. (11), into Eq. (13), ankle moment can be rewritten as;

$$T_{ank} = (a + L - x_2)x_1K_{yank} - (a + L - x_2)^2K_{yank}tan\theta \quad (14)$$

Also, substituting Eq. (9) into Eq. (14) for K_{yank}, the ankle moment can be expressed more clearly as Eq. (15);

$$T_{ank} = 2(a + L - x_2)x_1K\frac{L^2}{{x_2}^2} - 2(a + L - x_2)^2K\frac{L^2}{{x_2}^2}tan\theta \quad (15)$$

Differential equation of this ankle moment formulation in terms of θ gives the rotational stiffness of the ankle joint;

$$K_{\theta ank} = \frac{dT_{ank}}{d\theta} = -2K\frac{(a + L - x_2)^2L^2}{{x_2}^2cos\theta^2} \quad (16)$$

As given in Eq. (17), x_2 can be derived from Eq. (16). This equation can be used to calculate the required position of the output link to be controlled by the second motor (M2) for ankle joint stiffness adjustment.

$$x_2 = \frac{(a+L)L}{L+cos\theta.\sqrt{\frac{K_{\theta ank}}{2K}}} \quad (17)$$

Besides, Eq. (18) can be used to calculate the required position of the main motor (M1) for providing ankle joint moment;

$$x_1 = y_{ank} + \frac{T_{ank}}{(a + L - x_2)K_{yank}} \quad (18)$$

Substituting Eq. (9) into Eq. (18) for K_{ybilek}, the required equilibrium position of the controllable transmission ratio type actuator to be controlled by the main motor (M1) can be rewritten as Eq. (19);

$$x_1 = y_{ank} + \frac{T_{ank}.{x_2}^2}{2L^2(a+L-x_2)K} \quad (19)$$

Moreover, Substituting Eq. (10) into the Eq. (19) for y_{bilek}, the general form of the required equilibrium position of the actuator can be derived as Eq. (20);

$$x_1 = (a + L - x_1)tan\theta + \frac{T_{ank}.{x_2}^2}{2L^2(a + L - x_2)K} \quad (20)$$

Then, substituting Eqs. (20) and (10) into Eq.(8), the force applied by the main motor can expressed as Eq. (21);

$$F_1 = -2K\frac{L^2}{{x_2}^2}[(a + L - x_2).tan\theta] \quad (21)$$

The geometric relation between the spring side and ankle side of the force arm should be considered to calculate the force applied by the second motor (M2), and the free body diagram of the force arm is shown in Figure 6. In the figure, α and θ angles represent the angles between lever arm and force arm on the spring side, and between moment arm and force arm on the ankle joint side, respectively.

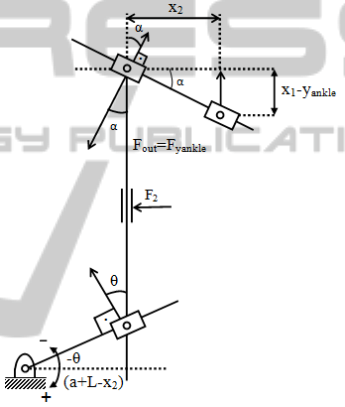

Figure 6: Free body diagram for the force arm of the controllable transmission ratio type actuator.

The sum of the horizontal forces can be equalized on the force arm ($\sum F_x = 0$) to calculate the force applied by the second motor (F_2). Thus, it can be formulated as Eq. (22);

$$F_2 = F_{ank}(\cos\alpha.\sin\alpha + \cos\theta\sin\theta) \quad (22)$$

In this equation, θ is equal to ankle joint angle and α can be expressed as Eq. (23) by considering the geometry on the free body diagram;

$$\alpha = arc\tan\left(\frac{x_1 - y_{ank}}{x_2}\right) \quad (23)$$

Finally, the total power requirement and total energy consumption of the controllable transmission ratio type actuator can be calculated by using Eqs. (24) and (25). The first and second terms of these equations represent the power requirement and energy consumption of the first and second motor, respectively. These equations will also be used to calculate the power requirement and energy

consumption of the other designs.

$$P = P_1 + P_2 = F_1.x_1 + F_2.\dot{x}_2 \quad (24)$$

$$W = \int |F_1\dot{x}_1|\,dt + \int |F_2\dot{x}_2|dt \quad (25)$$

2.2 Antagonistic Type Actuator

Two different series elastic actuators are connected with facing one another in the antagonistic design. In this design, the stiffness and the equilibrium point of the actuator could be adjusted by non-linear springs, which are simultaneously controlled by two different motors. The equivalent stiffness output characteristics of the variable stiffness actuators are desired to be linear. Therefore, quadratic non-linear springs should be used in the design of antagonistic type variable stiffness actuators for the linear adaptable compliance.

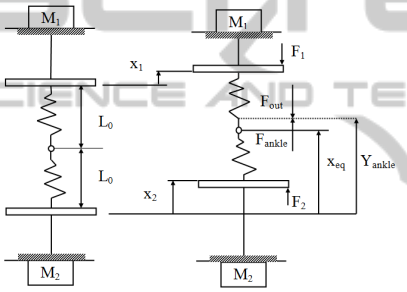

Figure 7: Schematic view of a linear antagonistic type variable stiffness actuator.

Figure 7 depicts a schematic view of a linear antagonistic design. Referring to Figure 7, x_{eq} is the equilibrium position of the actuator, y_{ank} is the linear displacement of ankle joint on the antagonistic type actuator. Also, x_{eq}, y_{ank}, F_{output}, F_{ank}, F_1, F_2, x_1, x_2, L_0 represents the equilibrium position of the actuator, position of the ankle, output force of the linear actuator, reaction force created by ankle over the actuator, force applied by the first motor, force applied by the second motor and free length of the springs used in the design, respectively. Under the assumption of that the springs are quadratic, ankle force will be equal to the difference of the forces created by the motors. Similar to the previous derivations, the positions and forces of the first and second motors are derived as Eqs. (26-29), respectively. The symbol K shows the stiffness rate of the quadratic spring model used in the antagonistic design ($F_{spring} = K.\Delta x^2$).

$$x_1 = \frac{F_{ank}}{K_{yank}} + y_{ank} + \frac{K_{yank}}{4K} \quad (26)$$

$$x_2 = \frac{F_{ank}}{K_{yank}} + y_{ank} - \frac{K_{yank}}{4K} \quad (27)$$

$$F_1 = K[y_{ank} - x_1]^2 \quad (28)$$

$$F_2 = K[x_2 - y_{ank}]^2 \quad (29)$$

2.3 Pre-tension Type Actuator

In the design of the pre-tension actuator (another name mechanically-controlled actuator) which is taken as an example in this study, there are two non-linear springs which are connected opposed to each other and compressed by only a one motor (M1). Therefore, the stiffness of the actuator on the connection point of the springs could be consistently adjusted by M1 and the second motor (M2) will be used to control the equilibrium point of the whole system. A schematic view is given in Figure 8 to figure out the pre-tension design example used in this study. In this schematic design example, M1 drives the twin ball-screw mechanism with double nut and compresses the opposed springs at the same amount. Therefore, the stiffness of the actuator could be easily changed by the equal displacement of the (quadratic) non-linear springs.

In Figure 8, x_{eq}, y_{ank}, F_{output}, F_{ank}, F_1, F_2, x_1, x_2, L_0 represents the equilibrium position of the actuator, position of the ankle, output force of the linear actuator, reaction force created by ankle over the actuator, force applied by the first motor, force applied by the second motor and free length of the springs used in the design, respectively. Note that the springs used in the pre-tension design were also quadratic ($F_{spring} = K.\Delta x^2$).

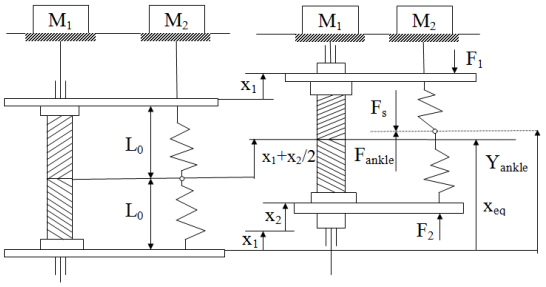

Figure 8: Schematic view of a pre-tension type variable stiffness actuator example.

With the similar derivations presented in the previous sections, the positions and forces of the first and second motors are derived as Eqs. (30-33), respectively.

$$x_1 = -\frac{F_{ank}}{K_{yank}} + y_{ank} - \frac{K_{yank}}{4K} \quad (30)$$

$$x_2 = \frac{K_{yank}}{2K} \quad (31)$$

$$F_1 = -F_{ank} \quad (32)$$

$$F_2 = K\left[-\frac{F_{ank}}{K_{yank}} + \frac{K_{yank}}{4K}\right]^2 \quad (33)$$

3 SIMULATION AND DISCUSSION

In this section, simulation results are presented in the case of in using ankle joint of antagonistic, pre-tension, controllable transmission type actuator designs and the results with these simulations are given. Before starting the simulation studies, biomechanics data are needed for the ankle with which the designs will be tested.

There are many biomechanic studies concerning human beings' lower body joints in the literature. In these studies, the walking patterns in different individuals' walking speed levels are observed by using markers positioned in joints and cameras. Thus, lower body joints' angles, speed and acceleration levels are obtained by processing these patterns. Furthermore, the mass and inertia of lower body joints for people with specific height and weight are also presented in the books related with biomechanics. Moment and power graphics for lower body joints during walking can be calculated by using angles, speed and acceleration levels obtained from the walking experiments in reverse dynamic equations.

Firstly, biomechanics data are needed for the angle and moment values of the ankle in simulation studies. The data provided by Bovi *et al*. study on bio-mechanics have been used in this study (Bovi, 2010). According to these data, ankle position angle and moment values of an optimum walking speed ($0.8 \leq$ walking speed/height ≤ 1) of an average adult, with 80 kg weight, are shown in Figure 9.

When the moment values given in Figure 9 are divided to the ankle angle values, in order to calculate the stiffness values of the ankle during walking, shown in Figure 10 have provided a stiffness value, which is really hard to happen. If these values are wanted to be obtained by any actuator whose stiffness can be changed, actuators, which can reach high stiffness values in a very short time, are required. This is really hard to apply, since it requires high levels of power. Therefore, Holgate *et al*. proposed to modify this stiffness graphic (Holgate, 2008).

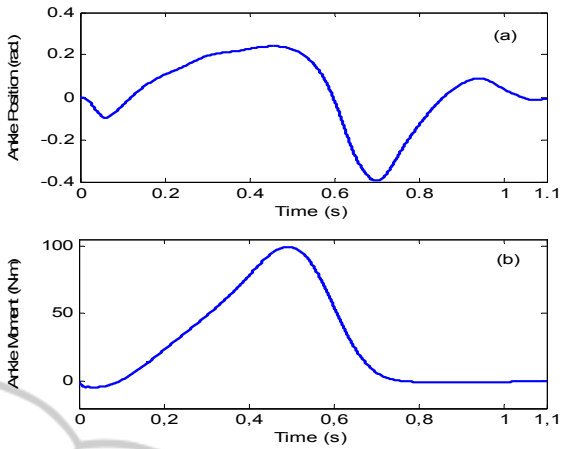

Figure 9: (a) Ankle angle and (b) ankle moment during one walking cycle.

This study aims to have reachable stiffness values by offsetting the ankle angle according to the recommended method. Stiffness value is near zero while the ankle is in swing phase in this method recommended by Holgate et al. It is inevitable to have unwanted oscillations when the stiffness value is zero in the swing phase of the ankle. Therefore, it is possible to prevent these unwanted oscillations by adding a second offset to the stiffness value obtained. Thus, the data in Figure 9 and the modified stiffness values obtained by using Eq.34 are obtained as given in Figure 10 (b).

$$K_{ankle} = A\frac{Tankle}{\theta_{ank} + \theta_{offset}} + K_{offset} \quad (34)$$

In Eq.34, K_{ankle} shows the stiffness value of the ankle to be used in the simulations, T_{ankle}, θ_{ankle}, θ_{offset}, K_{ankle} and A represent the moment of the ankle, the angle of the ankle, the offsetting in the angle of the ankle, the modified stiffness value of the ankle and tuning multiplier, respectively.

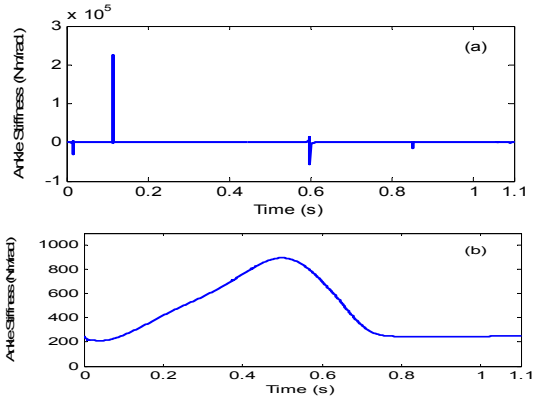

Figure 10: (a) Calculated stiffness values, (b) Modified stiffnesss values.

Obtaining the equation for the design of antagonistic, pre-tension and controllable transmission type actuator designs has been described in detail in Section 2.

Simulation tests for three different design have been run by using these equations in MATLAB Simulink®. In these simulation studies, the modified stiffness value given in Figure 10 (b) and ankle angle and torque values given in Figure 9 are taken as reference values. In the study for antagonistic and pre-tension actuators, quadratic spring model, and in the study for controllable transmission type actuator a linear spring model are used. Spring rate coefficients for quadratic and linear springs are taken to be K_{rate}=800 kN/m^2 and 3000 kN/m respectively. At the same time, slider-moment arm mechanism of a linear variable stiffness actuator used in an ankle joint was taken as (L) 10 cm.

In Figures 11 and 12, power requirement of motors used in each design and the amount of the energy spent by motors are presented. As can be analyzed power graph given in Figure 11, while in these three designs the first motors need 250W power, the second motors have quite different power needs. According to the reference simulation scenario, while in the antagonistic and pre-tension designs, second motor needs 100W power requirement, in the controllable transmission type actuator design needs 10W power requirement. Therefore, it is possible to work with smaller motors in the controllable transmission type actuator design.

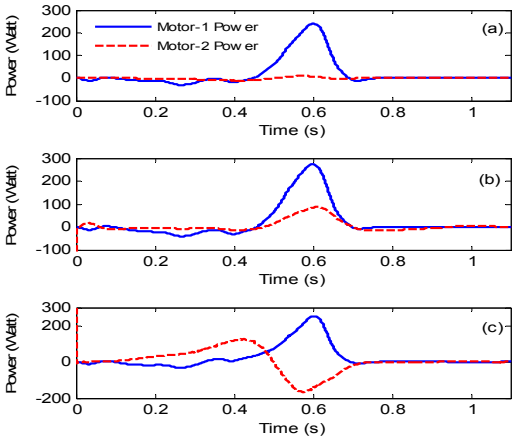

Figure 11: Power requirement; (a) controllable transmission type (b) antagonistic and (c) pre-tension type actuator designs.

In Figure 12, the energy levels consumed by motors similar to the graphics of power requirement are presented. As in power requirement graphics, even though the first motors of each three designs have similar energy consumption, there are significant differences in the second motors' energy consumption. The second motors consume 40J energy in pre-tension design, 15J energy in antagonistic design and about 3J energy in the controllable transmission type actuator design.

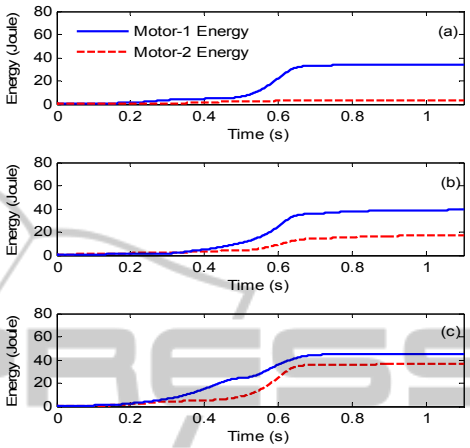

Figure 12: Consumed energy: (a) controllable transmission type (b) antagonistic and (c) pre-tension type actuator designs.

Lastly, for all three designs, the total energy consumed by motors are given in Figure 13. This graphic shows 80J energy in pre-tension design, 55J energy in antagonistic design and 37J energy in the controllable transmission type actuator design have been consumed during a walking cycle of an 80 kg person with the optimum speed (average speed) and the scenario of walking on a flat ground. The energy consumption difference between controllable transmission type actuator design and the other two designs are quite important for mobile human-like robots operated by batteries. Therefore, it concluded that in terms of energy consumption, it is much better to use controllable transmission type actuator design in exoskeleton robots.

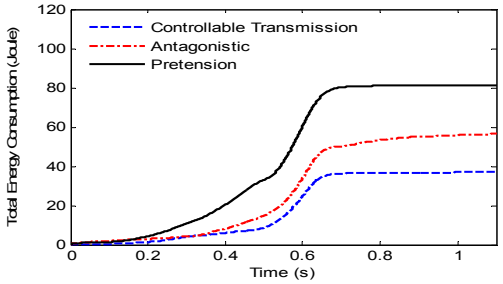

Figure 13: Total energy consumption.

4 CONCLUSIONS

In this study, first of all, equilibrium-controlled actuator, antagonistic-controlled actuator, structure-controlled actuator, mechanically-controlled actuator and controllable transmission ratio type actuator designs are presented in detail. Then, all equations have been derived for the design of an antagonistic, pre-tension and controllable transmission ratio type actuator designs. In the following section, these designs are compared in terms of energy consumption and power requirement at an optimal walking speed for ankle joint. According to the simulation results, as controllable transmission ratio type actuator requires less power and consumes less energy, it is more feasible than the antagonistic and pre-tension type designs for the joints of exoskeleton robots, orthoses, protheses and humanoid robots, which are supplied by the batteries.

ACKNOWLEDGEMENTS

The authors would like thank to TUBITAK (The Scientific and Technological Research Council of Turkey) for the financial support with a research project titled as “Design and control of a biomimetic exoskeleton robot”.

REFERENCES

Alexander R., 2010. Three uses of springs in legged locomotion. *Int. J. Robot. Res.* (Special Issue on Legged Locomotion), vol. 9, no. 2, pp. 53–61.

Bovi G., Rabuffetti M., Mazzoleni P. and Ferrarin M., 2010. A multiple-task gait analysis approach: kinematic, kinetic and EMG reference data for healthy young and adult subjects, Gait and Posture, vol: 33 pp.6-13.

Holgate M. A., Hitt J. K., Bellman R. D., Sugar T. G. and Hollander K.W., 2008. The SPARK (Spring Ankle with Regenerative kinetics) project: Choosing a DC motor based actuation method. *2nd IEEE RAS & EMBS International Conference on Biomedical Robotics and Biomechatronics*, pp.163-168.

Hollander K. W., Ilg R., Sugar T. G. and Herring D., 2006. An efficient robotic tendon for gait assistance. *J. Biomech. Eng.*,vol. 128, no. 5 pp. 788-91.

Jafari A., Tsagarakis N., Vanderborght B. and Caldwell D., 2010. A novel actuator with adjustable stiffness (AwAS). *IEEE/RSJ International Conference on Intelligent Robots and Systems*, pp.4201–4206.

Jafari A., Tsagarakis N. and Caldwell D. G., 2011. AwAS-II: A new actuator with adjustable stiffness based on the novel principle of adaptable pivot point and variable lever ratio. *IEEE International Conference on Robotics and Automation*, pp. 4638–4643.

Migliore S. A., Brown E. A., and DeWeerth S. P., 2005, Biologically inspired joint stiffness control. *IEEE Int. Conf. Robotics and Automation*, pp.4519–4524.

Pratt G. A., and Williamson M. M., 1995, Series elastic actuators,'' *in Proc. IEEE Int. Workshop on Intelligent Robots and Systems. Pittsburg*, USA, pp.399–406.

Van Ham R., Vanderborght B., Van Damme M., Verrelst B. and Lefeber D., 2007. MACCEPA, the mechanically adjustable compliance and controllable equilibrium position actuator: Design and implementation in a biped robot. Robot. Autonom. Syst., vol. 55, no. 10, pp. 761–768.

Vanderborght B., Albu-Schaeffer A., Bicchi A., Burdet E., Cald-well D., Carloni R., Catalano M., Ganesh G., Garabini M., Grioli G., Haddadin S., Jafari A., Laffranchi M., Lefeber D., Petit F., Stramigioli S., Grebenstein A., Tsagarakis N., Van Damme M., Van Ham R., Visser L. And Wolf S., 2012. Variable impedance actuators: Moving the robots of tomorrow. *IEEE/RSJ International Conference on Intelligent Robots and Systems*, pp. 5454-5455.